

Article

Mechanism and Chemoselectivity of Mn-Catalyzed Intramolecular Nitrene Transfer Reaction: C–H Amination vs. C=C Aziridination

Juping Wang ^{1,*}, Kangcheng Zheng ², Ting Li ¹ and Xiaojing Zhan ¹

¹ Department of Pharmaceutical Engineering, Guangdong Pharmaceutical University, Guangzhou 510006, China; wjplxg@163.com (T.L.); zhanxj0749@163.com (X.Z.)

² School of Chemistry, Sun Yat-sen University, Guangzhou 510275, China; ceszkc@mail.sysu.edu.cn

* Correspondence: jupingwang@gdpu.edu.cn; Tel.: +86-20-3935-2119

Received: 16 January 2020; Accepted: 26 February 2020; Published: 4 March 2020



Abstract: The reactivity, mechanism and chemoselectivity of the Mn-catalyzed intramolecular C–H amination versus C=C aziridination of allylic substrate *cis*-4-hexenylsulfamate are investigated by BP86 density functional theory computations. Emphasis is placed on the origins of high reactivity and high chemoselectivity of Mn catalysis. The N p orbital character of frontier orbitals, a strong electron-withdrawing porphyrazine ligand and a poor π backbonding of high-valent Mn^{III} metal to N atom lead to high electrophilic reactivity of Mn-nitrene. The calculated energy barrier of C–H amination is 9.9 kcal/mol lower than that of C=C aziridination, which indicates that Mn-based catalysis has an excellent level of chemoselectivity towards C–H amination, well consistent with the experimental the product ratio of amination-to-aziridination I:A (i.e., (Insertion):(Aziridination)) >20:1. This extraordinary chemoselectivity towards C–H amination originates from the structural features of porphyrazine: a rigid ligand with the big π -conjugated bond. Electron-donating substituents can further increase Mn-catalyzed C–H amination reactivity. The controlling factors found in this work may be considered as design elements for an economical and environmentally friendly C–H amination system with high reactivity and high chemoselectivity.

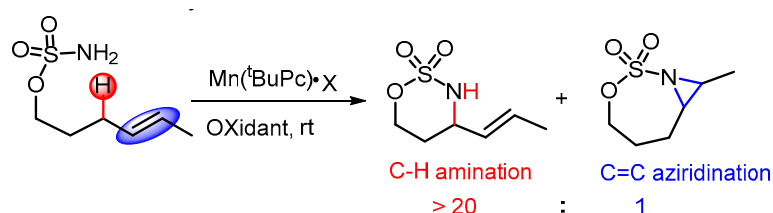
Keywords: mechanism; chemoselectivity; C–H amination; C=C aziridination; manganese

1. Introduction

Direct nitrene transfer (NT) reaction is an emerging and powerful method to convert C–H into C–N bonds from cheap and easily available starting materials [1–6]. Of these NT reactions catalyzed by organometallic complexes or metalloenzyme using metalloporphyrins as reactive center, the C(*sp*³)-H aminations of sulfamate esters are of immense interest because these reactions can install important structural motifs of therapeutic drugs, natural products and materials [7–11]. However, it is a particular challenge for amination of unsaturated sulfamate ester compounds such as allylic substrates since C=C may also react with nitrenoids to provide the aziridines, resulting in mixtures of amine and aziridine products [12–14]. Therefore, controlling the chemoselectivity of C–H bond amination vs. C=C bond aziridination is imperative to harness the full potential of this emerging method [15–19].

Noble metal such as rhodium [20–22], silver [23–25], ruthenium [26,27], palladium [28,29] and base metal such as iron [30–32], cobalt [33,34], copper [35,36] have been shown to accomplish C(*sp*³)-H aminations. Both of them, however, have some drawbacks in either reactivity or chemoselectivity for such catalysis. For example, noble metal rhodium catalysts are well known to catalyze the -NR group insertion reaction for its high reactivity but lack the chemoselectivity due to the competitive oxidation of π bonds (I (Insertion):A (Aziridination) = 1:1 by Rh₂(esp)₂ catalyst) [37]. Conversely,

base metal catalyst like [FePc] (Pc = phthalocyanine) have been attested the excellent chemoselectivity for intramolecular allylic amination over aziridination (I:A > 20:1) but poor chemical reactivity [13]. Moreover, this inverse correlation between reactivity and chemoselectivity universally exist in NT reactions. Therefore, obtaining a single product in both high effective and excellent chemoselective manner has been a long-standing goal in organic methodology. Excavating more effective metal catalysts to achieve this goal is going to be a significant trend. Recently, White and co-workers experimentally made a breakthrough wherein they found a novel manganese catalyst [Mn(tBuPc)] (tBuPc = tert-butylphthalocyanine) that exhibited prominent chemoselectivity (I:A > 20:1) while maintaining high reactivity observed with Rh₂-catalyst (Scheme 1) [38]. Both the reason for this reactivity-selectivity positive correlation and controlling factors for high chemoselectivity are still unknown up to now, and we infer that both of them might relate to the mechanism of the reaction and the structure of the Mn-catalyst.



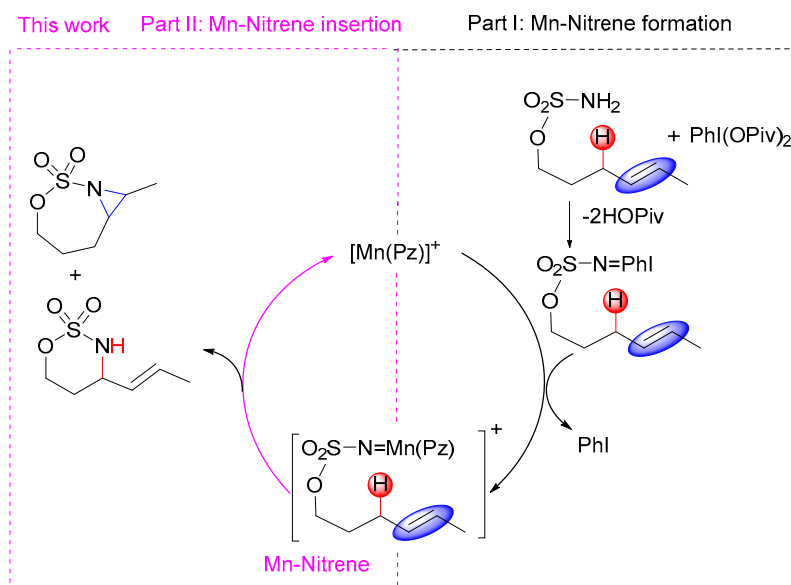
Scheme 1. C–H amination vs. C=C aziridination chemoselectivity by Mn-catalyst.

Computational chemistry plays an indispensable role in elucidating the reaction mechanism, unraveling the driving force for selectivity and designing new effective catalytic system [10,22,39–41]. Our group has engaged in theoretical investigations on mechanisms of C–N and C–C bond formations by means of C–H functionalization [42–45]. Herein, we performed detailed computational studies on the mechanisms of Mn-catalyzed intramolecular -NR insertion into C–H and C=C of allylic substrate, with an emphasis on the origins of reactivity and chemoselectivity for C–H amination vs. C=C aziridination. The insights drawn from Mn-phthalocyanine (porphyrin analogues) is expected to pave the way for the creation of new organometallic and metalloenzymatic catalysis system with high reactivity and high chemoselectivity.

2. Results and Discussion

In this work, porphyrazine (Pz) was utilized as a model for tBuPc. As seen in Scheme 2, it is accepted that the whole process of Mn-catalyzed reaction can be divided into two parts: the formation of Mn-nitrene intermediate (Part I) and the insertion of nitrene group into the C–H or C=C bond (Part II). Notably, metal-nitrene is a key species for nitrene delivery reaction. The competition of C–H amination vs. C=C aziridination depends solely on those reaction steps following the Mn-nitrene (vide the red box in Scheme 2). That is to say, chemoselectivity—the focus of this report—is irrespective of Part I. Thus our investigations on mechanism, reactivity and chemoselectivity for C–H amination vs. C=C aziridination start from the Mn-nitrene.

We use the following notations for the computed structures: ⁿNI_X (Mn-nitrene species), ⁿTS_{X-Y} (transition states), ⁿIM_{X-Y} (radical intermediates), ⁿPC_Y (products) and ⁿ[M] (Mn-based catalysts); where n = 1 and 3 for singlet and triplet spin state, respectively; X = CSS for closed-shell singlet, OSS for open-shell singlet; and Y = I and A for the C–H amination and C=C aziridination.



Scheme 2. Whole process for Mn-catalyzed intramolecular C-H amination and C=C aziridination. PhI(OPiv)₂ = Bis(tert-butylcarbonyloxy)iodobenzene.

2.1. Electronic Structure and Reactivity of Mn-Nitrene

In order to explain the high reactivity of Mn-nitrene species, three possible spin states of Mn-nitrene were investigated: closed-shell singlet state (CSS, ¹N_{ICSS}), open-shell singlet state (OSS, ¹N_{IOSS}) and triplet states (³NI). As shown in Figure 1, p_z, p_y and one of the sp-hybridization orbitals of the nitrenoid N atom overlap with d_{zz}, d_{yz} and d_{xz} orbitals of Mn center to form a σ- and two π- symmetry molecular orbitals, respectively. One may expect a qualitatively energetic ordering of Mn-nitrene as σ < π' < π'' < d_{xy} (Mn) < π''* < π'* < σ*. The electronic configuration of closed-shell singlet nitrene can be described as (σ)² (π')² (π'')² (d_{xy})² (π''*)⁰ (π'*)⁰ (σ*)⁰. The important frontier orbitals of Mn-nitrene are the nonbonding d_{xy} orbital, two antibonding π* orbitals and one antibonding σ* orbital. The π''* orbital is expected to be lower in energy than π'* orbital since π''* is also involved in the N-S bond of the bent nitrene unit leading to a poor overlap. The d_{xy} and π''* orbitals are close in energy, and the transition of one electron from d_{xy} to π''* orbital leads to the formations of open-shell singlet nitrene (two unpaired electrons of antiparallel spin) and triplet nitrene (two unpaired electrons of parallel spin). Obviously, Mn-N bond has a multiple-bond characteristic and its bond order would be 3 for ¹N_{ICSS} (one σ and two π bonds), 2.5 for ¹N_{IOSS} and ³NI (one σ, one π and half π bonds). Orbital overlap of p and d symmetry is not perfect in this system, especially for π'' orbital, therefore the actual Mn-N bonding is significantly mitigated. The length of Mn-N bond follows the trend: ¹N_{ICSS} (1.60 Å) < ¹N_{IOSS} (1.61 Å) << ³NI (1.70 Å). It is worth pointing out that a longer Mn-N bond is sterically accessible and dramatically facilitates the formation of the subsequent transition state, which is one of the factors contributing to the preference for triplet pathways (vide infra). More importantly, the π'* and π''* orbitals of ¹N_{ICSS}, ¹N_{IOSS} and ³NI have a large contribution from the N p orbital, which indicates that they can easily accept electrons from heterolytic or homolytic cleavages of σ_{C-H}/π_{C=C} bond of the substrates to trigger C-H amination/C=C aziridination reactions. In other words, Mn-nitrene has a strong electrophilic reactivity.

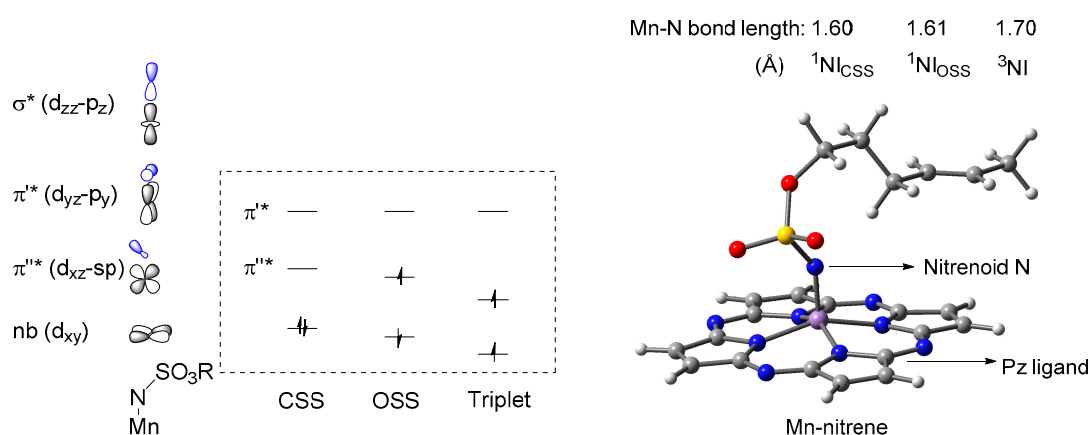


Figure 1. Molecular orbital ordering and optimized geometry of Mn–nitrene.

The other powerful factors influencing reactivity are the electronic effects from the Pz ligand and Mn^{III} metal. As shown in Figure 2, four stronger electronegativity of N vs. C atoms remarkably increases ability to accept electrons of Pz ligand, makes a less electronic Mn–N reactive center and lead to a Mn(Pz)-nitrene with higher electrophilic reactivity than Mn(Por)-nitrene, consistent with observed experiments [38]. In metal-center terms, Mn^(III) (d^4) has less d-electrons compared to Fe^(III) (d^5), which indicates a poorer π -backbonding effect from Mn^(III) to N¹ and a more electron-deficient nitrenoid N atom, thus a stronger electrophilicity for Mn(Pz) than Fe(Pz).

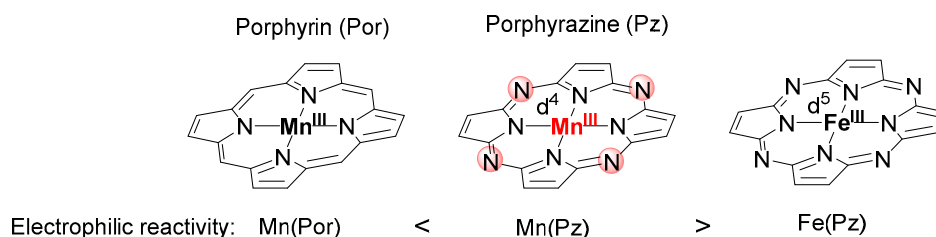


Figure 2. Effects of the Pz ligand and Mn^{III} on reactivity of Mn-nitrene.

The N p orbital character of frontier orbitals, a strong electron-withdrawing porphyrazine ligand and a high-valent Mn^{III} metal lead to high electrophilic reactivity of Mn-nitrene. This is supported by the relative experimental results that both Mn(Pz)-catalyzed intramolecular C–H amination/C=C aziridination can be executed at approximately regular temperature.

2.2. Mechanistic Investigation on C–H Amination and C=C Aziridination

One of the main advantages for Mn-based catalyst is its excellent chemoselectivity towards C–H amination, and this high chemoselectivity is related to reaction mechanism. Here we present mechanistic investigation findings of the C–H amination and C=C aziridination. All potential energy surfaces are shown in Figure 3 and optimized geometries are depicted in Figure 4 for transition states and S1 for other species. For the convenience of discussion, Figure 3 also presents labels of important atoms of all species involved in the amination and aziridination pathways.

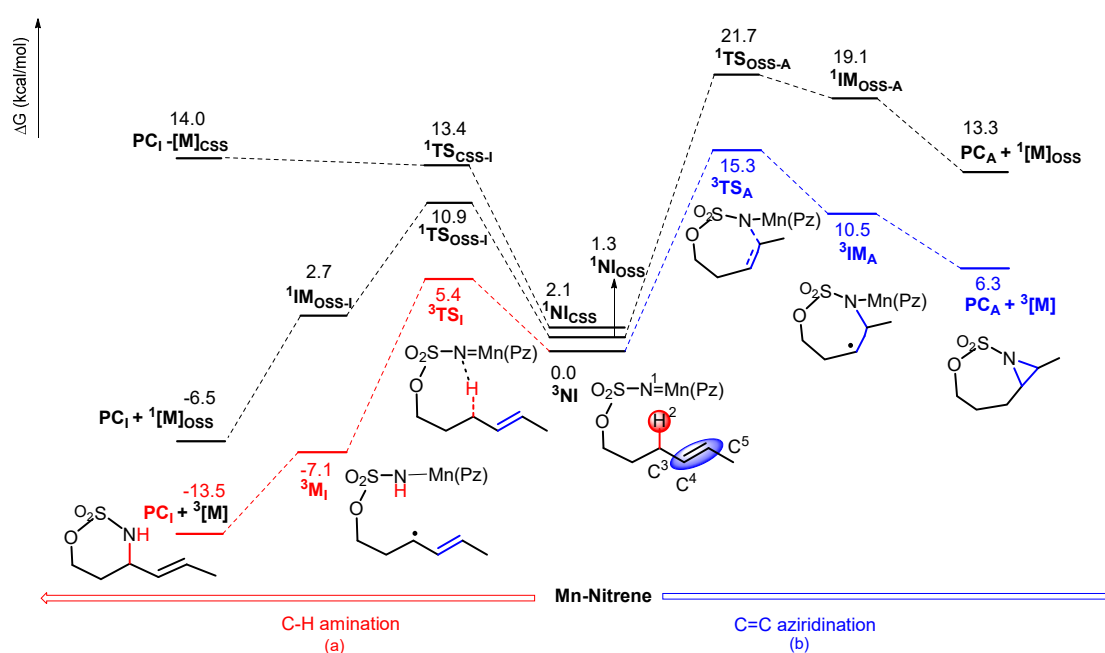


Figure 3. Free energy profile (in gas-phase) of possible pathways for (a) C–H bond amination and (b) C=C bond aziridination. Free energies are calculated at the BP86/6-31+G(d,p)-LANL08(f)//BP86/6-31G(d,p)-LANL08(f) level of theory.

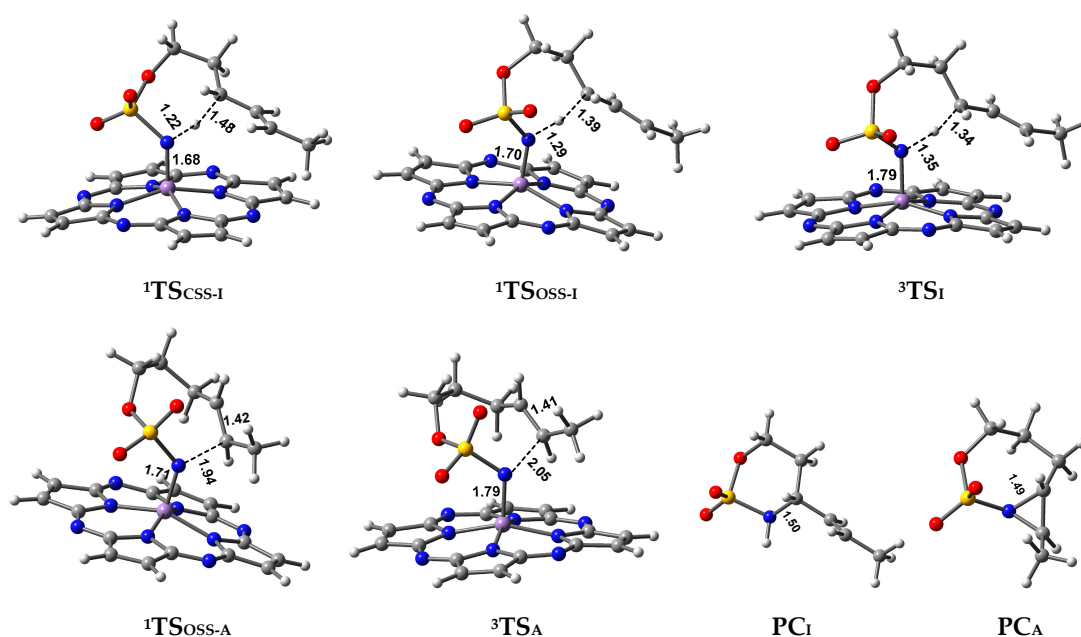


Figure 4. Optimized structures with geometrical parameters (bond lengths in Å) of the key species in the reaction pathways.

2.2.1. C–H Amination Mechanism

For Mn-catalyzed intramolecular C–H amination reaction, there are three possible pathways: closed-shell singlet pathway, open-shell singlet pathway and triplet pathway.

Closed-Shell Singlet (CSS) Pathway of Amination

For nitrene $^1\text{NI}_{\text{CSS}}$, its π^{**} or π^* orbitals, as analyzed above, have a significant N p component and can accept two electrons from the heterolytic cleavage of $\sigma_{\text{C3-H2}}$ to promote the singlet pathway.

This heterolytic cleavage of C^3-H^2 with the negative hydrogen transferring process is supported by calculated NBO charges. As ${}^1NI_{CSS} \rightarrow {}^1TS_{CSS-I} \rightarrow PC_I$, the total NBO negative charges of the $C^3-C^4-C^5$ moiety decrease gradually ($-0.787 \text{ e} \rightarrow -0.549 \text{ e} \rightarrow -0.475 \text{ e}$), while negative charges for nitrenoid N^1 atom increase correspondingly ($-0.263 \text{ e} \rightarrow -0.518 \text{ e} \rightarrow -0.844 \text{ e}$). In structure terms, the distances of $C^3 \cdots H^2$, $N^1 \cdots H^2$, and $C^3 \cdots N^1$ in the transition state ${}^1TS_{CSS-I}$ are 1.48, 1.22, and 2.67 Å, respectively, indicative of a breaking $C^3 \cdots H^2$ bond with forming $N^1 \cdots H^2$ and $C^3 \cdots N^1$ bonds (Figure 4). Moreover, in the subsequent six-membered ring amination product 1PC_I , the bond lengths of N^1-H^2 and C^3-N^1 are 1.03 and 1.50 Å, respectively, suggesting that both N^1-H^2 and C^3-N^1 bonds are indeed completely formed. All the above bond distances show that the cleavage of the C–H bond and the formations of the N^1-H^2 and C^3-N^1 bonds proceed in a concerted manner. Therefore, the singlet intramolecular amination mechanism of Manganese catalysis (${}^1NI_{CSS} \rightarrow {}^1TS_{CSS-I} \rightarrow PC_I$) can be described as a concerted hydride-transfer pathway.

Triplet and OSS Pathway of Amination

OSS and triplet pathways is analogous. Herein, the triplet pathway is given as an example to illustrate the nature of triplet and OSS mechanisms. In contrast to CSS pathway, the triplet pathway begins in the triplet 3NI . Its π^{**} or π^* orbital with large N p character accept one electron from the homolytic cleavage of the $\sigma_{C^3-H^2}$ bond to form N^1-H^2 bond via transition state 3TS_I wherein the calculated distances of $C^3 \cdots H^2$ and $N^1 \cdots H^2$ are 1.34 and 1.35 Å, respectively. The other electron of the homolytic cleavage is left on C^3 atom, leading to the formation of a radical intermediate 3IM_I with a good p– π conjugation. This $\sigma_{C^3-H^2}$ bond homolytic process is supported by a gradually increasing trend of spin populations of the $C^3-C^4-C^5$ moiety (-0.113 e for ${}^3NI \rightarrow -0.378 \text{ e}$ for ${}^3TS_I \rightarrow -0.406 \text{ e}$ for 3IM_I) and decreasing of spin populations on N^1 atom (-0.204 e for ${}^3NI \rightarrow -0.133 \text{ e}$ for ${}^3TS_I \rightarrow 0.037 \text{ e}$ for 3IM_I). Subsequently, C^3 and N^1 atoms in 3IM_I recombine to form the final amination product PC_I with the dissociation of triplet catalyst ${}^3[Mn]$. In conclusion, Mn-catalyzed triplet amination pathway (${}^3NI \rightarrow {}^3TS_I \rightarrow {}^3IM_I \rightarrow PC_I$) can be described as H-abstraction/radical recombination process. The overall process along this triplet pathway is exothermic by -13.5 kcal/mol .

Preference of Singlet–Triplet Pathway for C–H Amination

A look at the Figure 3 shows that the energetic ordering of the three transition states is 3TS_I (5.4 kcal/mol) < ${}^1TS_{OSS-I}$ (10.9 kcal/mol) < ${}^1TS_{CSS-I}$ (13.4 kcal/mol). The energy barrier of triplet 3TS_I is the lowest among three transition states, which suggests that triplet pathway is greatly favored over the closed-shell and open-shell singlet pathways for allylic C–H amination reactions. Firstly, in triplet 3TS_I , an unpaired electron from the homolytic cleavage of σ_{C-H} can delocalize to the adjacent C=C by a p– π conjugation, which stabilizes triplet 3TS_I . Secondly, as seen from the C^3-H^2 bond length (3TS_I (1.34 Å) < ${}^1TS_{OSS-I}$ (1.39 Å) < ${}^1TS_{CSS-I}$ (1.48 Å), see Figure 4), the least breakage extent of C^3-H^2 lead to the lowest barrier for 3TS_I . Finally, a longest Mn–N bond (3TS_I (1.79 Å) > ${}^1TS_{OSS-I}$ (1.70 Å) > ${}^1TS_{CSS-I}$ (1.68 Å)) reduces the steric repulsion between rigid Pz ligand and the sulfamate reactant, and thus lowers the energy of 3TS_I .

2.2.2. C=C Aziridination Mechanism

Triplet and OSS Pathways of Aziridination

As mentioned above, π^{**} or π^* orbitals for triplet Mn-nitrene have a significant N p orbital character. These orbitals can accept not only the σ electron from C–H bond cleavage but also the π electron from C=C bond cleavage leading to a competitive aziridination reaction. Despite all the efforts to search for a concerted closed-shell singlet transition state for C=C bond aziridination, it was unable to be located. We infer that a large steric repulsion between Mn-catalyst and sulfamate substrate fragments results in the absence of the concerted CSS transition state for aziridination mechanism. Open-shell singlet and triplet pathways for aziridination were located.

In triplet aziridination pathways (${}^3\text{NI} \rightarrow {}^3\text{TS}_A \rightarrow {}^3\text{IM}_A \rightarrow \text{PC}_A$, Figure 3), the first step is that π^* or π^* orbitals of triplet Mn-nitrene ${}^3\text{NI}$ accept one electron from π_{p-p} homolytic cleavage of $\text{C}^4=\text{C}^5$ bond to form a new N^1-C^5 bond via the transition state ${}^3\text{TS}_A$, while the other electron is left on C^4 center. As a result, the radical intermediate ${}^3\text{IM}_A$ is formed. This homolytic cleavage process is supported by a gradually increasing trend of β -spin population on the C^4 atom ($|-0.039\text{ e}|$ for ${}^3\text{NI} \rightarrow |-0.430\text{ e}|$ for ${}^3\text{TS}_A \rightarrow |-0.686\text{ e}|$ for ${}^3\text{IM}_A$) and decreasing trend of spin populations on N^1 atom ($|-0.204\text{ e}|$ for ${}^3\text{NI} \rightarrow |-0.139\text{ e}|$ for ${}^3\text{TS}_A \rightarrow |0.084\text{ e}|$ for ${}^3\text{IM}_I$). In ${}^3\text{IM}_A$, there are three unpaired α -spin electrons on the Mn center (2.469 e) and a β -spin electron on the C^4 atom (-0.686 e). Subsequently, one of α electrons of Mn center transfers to N^1 atom and couples with the β electron of C^4 atom to form the C–N bond with the dissociation of triplet catalyst ${}^3[\text{M}]$. As a result, the final aziridine product PC_A is obtained. In conclusion, Mn-catalyzed triplet aziridination pathway can be characterized as radical addition/recombination process. This intramolecular aziridination mechanism by $[\text{Mn}(\text{Pz})]^+$ is similar to the intermolecular by $[(\text{MeCN})(\text{L})\text{Mn-NCMe}]^-$ [33]. The overall process along this pathway (${}^3\text{NI} \rightarrow {}^3\text{TS}_A \rightarrow {}^3\text{IM}_A \rightarrow \text{PC}_A$) is exothermic by -28.5 kcal/mol .

As shown in Figure 3, the open-shell singlet pathway proceeds as the two-step mechanism similar to triplet pathways. Through transition state ${}^1\text{TS}_{\text{OSS-A}}$, nitrenoid N atom of ${}^1\text{NI}_{\text{OSS}}$ accept one electron from π_{p-p} homolytic cleavage of $\text{C}^4=\text{C}^5$ bond to form the intermediate ${}^1\text{IM}_{\text{OSS-A}}$, which is then followed by radical recombination to yield the aziridine product PC_A with the dissociation of open-shell singlet catalyst ${}^1[\text{M}]_{\text{OSS}}$.

The breaking extent of $\text{C}^4=\text{C}^5$ bond in ${}^3\text{TS}_A$ is less than that in ${}^1\text{TS}_{\text{OSS-A}}$ (3.7% vs. 4.9%), while the forming $\text{N}^1\cdots\text{C}^5$ bond distance in ${}^3\text{TS}_A$ is longer than that in ${}^1\text{TS}_{\text{OSS-A}}$ (2.053 Å vs. 1.940 Å), both of which reveal that the triplet ${}^3\text{TS}_A$ has a more reactant-like character than open-shell singlet ${}^1\text{TS}_{\text{OSS-A}}$, and thus a lower activation barrier (15.3 vs. 21.7 kcal/mol). In other words, the triplet pathway (${}^3\text{NI} \rightarrow {}^3\text{TS}_A \rightarrow {}^3\text{IM}_A \rightarrow \text{PC}_A$) is preferable over the open-shell singlet one for Mn-catalyzed C=C bond aziridination reaction. The overall process along this triplet pathway is endothermic by 6.3 kcal/mol.

Alternatively, $\text{C}^4=\text{C}^5$ Aziridination might proceed via triplet transition state ${}^3\text{TS}_{A-C4}$ in which C^4 center is initially attacked by triplet nitrenoid N^1 atom. The calculated energy barrier of ${}^3\text{TS}_{A-C4}$ is 6.9 kcal/mol higher than that of ${}^3\text{TS}_A$ (22.2 vs. 15.3 kcal/mol), indicating that $\text{C}^4=\text{C}^5$ aziridination occurs via the transition state ${}^3\text{TS}_A$ rather than via ${}^3\text{TS}_{A-C4}$.

2.3. Chemoselectivity of C–H Amination vs. C=C Aziridination

As shown in Figure 3, ${}^3\text{TS}_I$ is 9.9 kcal/mol lower in energy than ${}^3\text{TS}_A$ (5.4 vs. 15.3 kcal/mol) while triplet amination and aziridination pathways are exothermic by -13.5 kcal and endothermic by 6.3 kcal/mol, respectively, which indicates that C–H amination significantly is both kinetically and thermodynamically favorable over C=C aziridination for Mn-catalyzed system, excellently consistent with the experimental I:A > 20:1. This extraordinary chemoselectivity toward C–H amination can be explained by the following. Firstly, the $p-\pi$ conjugation in triplet ${}^3\text{TS}_I$ lowers the activation energy of the amination. This role of the $p-\pi$ conjugation in the selectivity of intramolecular reactions is also reflected on the intermolecular: aromatic over aliphatic alkenes in aziridination reactions catalyzed by $[(\text{MeCN})(\text{L})\text{Mn-NCMe}]^-$ [33]. Secondly, the Pz is a π -conjugated macrocyclic ligand with good planarity and strong rigidity. It is difficult for Pz to make a pocket-like space to accommodate other approaching atoms in the reaction process. Namely, nitrenoid N atom above Pz is sterically inaccessible. As seen in Figure 4, 8-membered ring moiety of ${}^3\text{TS}_A$ “lie” above the Pz plane whereas moiety of ${}^3\text{TS}_I$ “stand” above the Pz plane. Obviously, “lie” mode has a much larger steric repulsive-force between Pz ligand and sulfamate substrate compared to “stand” mode, which greatly lead to a higher energy barrier for ${}^3\text{TS}_A$ than for ${}^3\text{TS}_I$. Thermodynamically, a 7-membered ring and a 3-membered ring in the aziridination product PC_A indicate much larger tension than 6-membered ring in amination product PC_I . It further inhibits C=C aziridination competition.

It is worth pointing out that the planar and rigid character in structure for Pz ligand plays a critical role in inhibiting C=C aziridination to increase I:A ratio. This directed effect is also observed

in Co-catalyzed allylic C–H amination vs. C=C aziridination system where the experimental I:A chemoselectivity is >99:1 and all utilized Co-catalysts involve a porphyrin framework with planar and rigid character as Pz ligand [18]. One may consider this sterically directed effect as a design element for a new high chemoselectivity system. To obtain a single amination product for allylic substrate, metal-based catalyst with a rigid planar ligand is a more suitable candidate.

2.4. Substitution Effects on the Aminations

To find out the electronic nature of the transition state for C–H cleavage of amination reaction by Mn-catalyst, we extend our research to the effects of substituents with different electronic property for Mn-catalyzed C–H aminations. In this section, the nitrene and transition state were denoted as **R–Bn–³NI** and **R–Bn–³TS**, respectively, where R = CH₃, H and F (Figure 5). The computed activation energy are shown in Table 1. A gradually increasing trend of activation energy such as **CH₃–Bn–³TS** (7.2 kcal/mol) < **H–Bn–³TS** (8.7 kcal/mol) < **F–Bn–³TS** (9.1 kcal/mol) intimates that the electron-donating group tends to increase the reactivity for C–H amination whereas electron-withdrawing group makes a slight deactivation, which is consistent with experimentally negative Hammett ρ value (ρ = –0.88) [38]. The reasonable explanation is that electron-donating –CH₃ can increase electron density of benzylic C–H bond, and then the increased electron-rich character of benzylic C–H bond is more readily attacked by the electrophilic nitrene N atom. This substituent effect is analogous to Rh₂-based system [42].

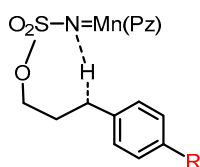


Figure 5. Substitution effects on the aminations.

Table 1. Comparison of active free energy in solvent (kcal/mol) of the C–H aminations for R = CH₃, H and F. Free energies are calculated at the BP86/6-31+G(d,p)-LANL08(f)//BP86/6-31G(d,p)-LANL08(f) level of theory.

Species	$\Delta G(\text{CH}_3)$	$\Delta G(\text{H})$	$\Delta G(\text{F})$
R–Bn–³NI	0.0	0.0	0.0
R–Bn–³TS	7.2	8.7	9.1

In summary, it is a good choice introducing some electron-donating groups such as OCH₃, OH, or CH₃ on the substrate to further improve aminating reactivity by Mn-catalyst.

3. Computational Details

All calculations were performed by employing the pure functional BP86 [46] level of theory, which has been shown to give reliable results for NT systems including multiple spin-state pathways [11,47–50]. All reported structures were fully optimized without any geometry constraints where the 6-31G(d,p) basis sets were utilized for C, H, N, O and S atoms, and LANL08(f) basis sets with the corresponding effective core potentials (ECPs) were used for Mn atom (referred to below as basis sets BS1) [51–53]. All transition states were confirmed according to the vibrational mode of their one and only imaginary negative frequency (see Supporting materials for more details). Broken symmetry calculations were employed for all open-shell singlet species and the stability of wave functions were confirmed. To improve energetics of the reported structures, we performed single-point energy calculations at the BP86 level of theory combined with 6–311+G(df,p) basis sets for C, H, N, O and S atoms, and LANL08(f) basis sets for Mn-center (referred to below as basis sets BS2). At the BP86/BS2 level of

theory, solvent effects were estimated in benzene by means of the solvation model based on density (SMD) [54] and corresponding free energies are shown in the Supplementary materials.

All calculations were performed by the Gaussian 09 suite of programs [55]. In order to enhance the calculation accuracy, the integration grid and 2-electron integral accuracy were set to 'UltraFine' and '10⁻¹²', respectively. The reported thermodynamic data were computed at 298.15K temperature and 1 atm pressure.

4. Conclusion

This work presents a theoretical investigation on the reactivity, mechanism and chemoselectivity of Mn-catalyzed intramolecular nitrene transfer reaction: C–H bond amination vs. C=C bond aziridination. The origin of high reactivity and high chemoselectivity were explored in detail. We also studied the influence of substituents on the reactivity of Mn-catalyzed C–H amination.

(1) Axial Mn=N bond has an obvious multiple bonding character. A large N p orbital component of frontier orbitals indicates that nitrenoid N atom can readily accept electrons of C–H or C=C bond and thus Mn-nitrene has an electrophilic reactivity. A good electron-withdrawing Pz ligand and a poor π backbonding of Mn^{III} metal to N atom lead to increased electron-deficiency at the nitrenoid N center, which further enhances electrophilic reactivity of Mn-nitrene.

(2) Mn-catalyzed C–H amination and C=C aziridination both proceed as a triplet stepwise pathway involving H-abstraction/radical recombination for the former and radical addition/radical recombination for the latter to produce singlet amination and aziridination product, respectively.

(3) For allylic substrate *cis*-4-hexenylsulfamate, the calculated energy barrier of C–H amination is 9.9 kcal/mol higher than that of C=C aziridination, which indicates that Mn-nitrene has a very high chemoselectivity towards C–H amination, well consistent with the experimental I:A > 20:1. This extraordinary chemoselectivity originates from structurally rigid and planar characters of Pz ligand which results in a large steric repulsion between Pz and sulfamate substrate moieties in the aziridination transition state and thus greatly inhibiting C=C aziridination to increase the I:A ratio. This sterically directed effects may be considered as a design element for a new high chemoselectivity system. To obtain a single amination product for allylic substrate, Metal-based catalyst with rigid planar ligand is a suitable candidate.

(4) Electron-donating substituents can further increase Mn-catalyzed C–H amination reactivity. It is a good choice through introducing some electron-donating groups such as OCH₃, OH, or CH₃ in appropriate position of the substrate to increase C–H amination efficiency.

Mn base metal is ten million times more abundant than Rh noble metal, while owning high reactivity and chemoselectivity. Our results will greatly facilitate future sustainable chemical catalysis and biocatalysis related to nitrene transfer reactions.

Supplementary Materials: Supplementary materials associated with this article can be found in the online version <http://www.mdpi.com/2073-4344/10/3/292/s1>.

Author Contributions: Data curation, J.W. and K.Z.; funding acquisition, J.W.; project administration, J.W.; visualization, J.W.; writing-original draft, J.W. and T.L.; writing-review and editing, J.W. and X.Z. All authors have read and agreed to the published version of the manuscript.

Funding: This research was funded by Natural Science Foundation of Guangdong Province, grant number 2017A030313044 and Special Program for Applied Research on Super Computation of the NSFC-Guangdong Joint Fund (the second phase). The APC was funded by Natural Science Foundation of Guangdong Province, grant number 2017A030313044.

Acknowledgments: The authors thank the National Supercomputing Center in GuangZhou for providing the computational resources and Natural Science Foundation of Guangdong Province, China (2017A030313044) and Special Program for Applied Research on Super Computation of the NSFC-Guangdong Joint Fund (the second phase) for financial support.

Conflicts of Interest: The authors declare no conflict of interest.

Abbreviations

vs.	versus
Mn	Manganese
NT	nitrene transfer
I	Insertion
A	Aziridination
Pc	phthalocyanine
tBuPc	tert-butylphthalocyanine
Pz	Porphyrazine
CSS	closed-shell singlet state
OSS	open-shell singlet state
Por	Porphyrin
NBO	Natural Bond Orbital
ECPs	effective core potentials
BS	basis sets
IRC	Intrinsic reaction coordinate
SMD	solvation model based on density

References

1. Davies, H.M.L.; Morton, D. Collective approach to advancing C-H functionalization. *ACS Cent. Sci.* **2017**, *3*, 936–943. [[CrossRef](#)] [[PubMed](#)]
2. Darses, B.; Rodrigues, R.; Neuville, L.; Mazurais, M.; Dauban, P. Transition metal-catalyzed iodine(III)-mediated nitrene transfer reactions: Efficient tools for challenging syntheses. *Chem. Commun.* **2017**, *53*, 493–508. [[CrossRef](#)]
3. Park, Y.; Kim, Y.; Chang, S. Transition metal-catalyzed C-H amination: Scope, mechanism, and applications. *Chem. Rev.* **2017**, *117*, 9247–9301. [[CrossRef](#)]
4. Clark, J.R.; Feng, K.; Sookezian, A.; White, M.C. Manganese-catalysed benzylic C(sp³)-H amination for late-stage functionalization. *Nat. Chem.* **2018**, *10*, 583–591. [[CrossRef](#)] [[PubMed](#)]
5. Degenaro, L.; Trinchera, P.; Luisi, R. Recent advances in the stereoselective synthesis of aziridines. *Chem. Rev.* **2014**, *114*, 7881–7929. [[CrossRef](#)]
6. Yang, Y.; Cho, I.; Qi, X.; Liu, P.; Arnold, F.H. An enzymatic platform for the asymmetric amination of primary, secondary and tertiary C(sp³)-H bonds. *Nat. Chem.* **2019**, *11*, 987–993. [[CrossRef](#)] [[PubMed](#)]
7. Prier, C.K.; Zhang, R.K.; Buller, A.R.; Chen, S.B.; Arnold, F.H. Enantioselective, intermolecular benzylic C-H amination catalysed by an engineered iron-haem enzyme. *Nat. Chem.* **2017**, *9*, 629–634. [[CrossRef](#)]
8. Roizen, J.L.; Harvey, M.E.; Du Bois, J. Metal-catalyzed nitrogen-atom transfer methods for the oxidation of aliphatic C-H bonds. *Acc. Chem. Res.* **2012**, *45*, 911–922. [[CrossRef](#)]
9. Chiappini, N.D.; Mack, J.B.C.; Du Bois, J. Intermolecular sp³ C-H amination of complex molecules. *Angew. Chem. Int. Ed. Engl.* **2018**, *18*, 4956–4959. [[CrossRef](#)]
10. Huang, M.; Yang, T.; Paretsky, J.D.; Berry, J.F.; Schomaker, J.M. Inverting steric effects: Using “attractive” noncovalent interactions to direct silver-catalyzed nitrene transfer. *J. Am. Chem. Soc.* **2017**, *139*, 17376–17386. [[CrossRef](#)]
11. Goswami, M.; Lyaskovskyy, V.; Domingos, S.R.; Buma, W.J.; Woutersen, S.; Troeppner, O.; Ivanović-Burmazović, I.; Lu, H.; Cui, X.; Zhang, X.P.; et al. Characterization of porphyrin-Co(III)-‘nitrene radical’ species relevant in catalytic nitrene transfer reactions. *J. Am. Chem. Soc.* **2015**, *137*, 5468–5479. [[CrossRef](#)] [[PubMed](#)]
12. Harvey, M.E.; Musaev, D.G.; Du Bois, J. A diruthenium catalyst for selective, intramolecular allylic C-H amination: Reaction development and mechanistic insight gained through experiment and theory. *J. Am. Chem. Soc.* **2011**, *133*, 17207–17216. [[CrossRef](#)]
13. Paradine, S.M.; White, M.C. Iron-catalyzed intramolecular allylic C-H amination. *J. Am. Chem. Soc.* **2012**, *134*, 2036–2039. [[CrossRef](#)] [[PubMed](#)]

14. Weatherly, C.; Alderson, J.M.; Berry, J.F.; Hein, J.E.; Schomaker, J.M. Catalyst-controlled nitrene transfer by tuning metal:ligand ratios: Insight into the mechanisms of chemoselectivity. *Organometallics* **2017**, *36*, 1649–1661. [[CrossRef](#)]
15. Li, J.; Cisar, J.S.; Zhou, C.-Y.; Vera, B.; Vera, W.H.; Rodríguez, A.D.; Cravatt, B.F.; Romo, D. Simultaneous structure–activity studies and arming of natural products by C-H amination reveal cellular targets of eupalmerin acetate. *Nat. Chem.* **2013**, *5*, 510–517. [[CrossRef](#)]
16. Dolan, N.S.; Scamp, R.J.; Yang, T.; Berry, J.F.; Schomaker, J.M. Catalyst-controlled and tunable, chemoselective silver-catalyzed intermolecular nitrene transfer: Experimental and computational studies. *J. Am. Chem. Soc.* **2016**, *138*, 14658–14667. [[CrossRef](#)]
17. Zalatan, D.N.; Du Bois, J. A chiral rhodium carboxamidate catalyst for enantioselective C-H amination. *J. Am. Chem. Soc.* **2008**, *130*, 9220–9221. [[CrossRef](#)]
18. Lu, H.; Jiang, H.; Hu, Y.; Wojtas, L.; Zhang, X.P. Chemoselective intramolecular allylic C-H amination versus C=C aziridination through Co(II)-based metalloradical catalysis. *Chem. Sci.* **2011**, *2*, 2361–2366. [[CrossRef](#)]
19. Zhang, X.; Xu, H.; Zhao, C. Mechanistic investigation of dirhodium-catalyzed intramolecular allylic C-H amination versus alkene aziridination. *J. Org. Chem.* **2014**, *79*, 9799–9811. [[CrossRef](#)]
20. Rodrigues, R.; Lazib, Y.; Maury, J.; Neuville, L.; Leboeuf, D.; Dauban, P.; Darses, B. Approach to pactamycin analogues using rhodium(II)-catalyzed alkene aziridination and C(sp³)-H amination reactions. *Org. Chem. Front.* **2018**, *5*, 948–953. [[CrossRef](#)]
21. Paudyal, M.P.; Adebesein, A.M.; Burt, S.R.; Ess, D.H.; Ma, Z.; Kürti, L.; Falck, J.R. Dirhodium-catalyzed C-H amination using hydroxylamines. *Science* **2016**, *353*, 1144–1147. [[CrossRef](#)]
22. Varela-Álvarez, A.; Yang, T.; Jennings, H.; Kornecki, K.P.; Macmillan, S.N.; Lancaster, K.M.; Mack, J.B.C.; Du Bois, J.; Berry, J.F.; Musaev, D.G. Rh₂(II,III) catalysts with chelating carboxylate and carboxamidate supports: Electronic structure and nitrene transfer reactivity. *J. Am. Chem. Soc.* **2016**, *138*, 2327–2341. [[CrossRef](#)]
23. Alderson, J.M.; Corbin, J.R.; Schomaker, J.M. Tunable, chemo- and site-selective nitrene transfer reactions through the rational design of silver(I) catalysts. *Acc. Chem. Res.* **2017**, *50*, 2147–2158. [[CrossRef](#)] [[PubMed](#)]
24. Scamp, R.J.; Jirak, J.G.; Dolan, N.S.; Guzei, I.A.; Schomaker, J.M. A general catalyst for site-selective C(sp³)-H bond amination of activated secondary over tertiary alkyl C(sp³)-H bonds. *Org. Lett.* **2016**, *18*, 3014–3017. [[CrossRef](#)] [[PubMed](#)]
25. Ju, M.; Weatherly, C.D.; Guzei, I.A.; Schomaker, J.M. Chemo- and enantioselective intramolecular silver-catalyzed aziridinations. *Angew. Chem.* **2017**, *129*, 10076–10080. [[CrossRef](#)]
26. Manca, G.; Gallo, E.; Intrieri, D.; Mealli, C. DFT mechanistic proposal of the ruthenium porphyrin-catalyzed allylic amination by organic azides. *ACS Catal.* **2014**, *4*, 823–832. [[CrossRef](#)]
27. Qin, J.; Zhou, Z.; Cui, T.; Hemming, M.; Meggers, E. Enantioselective intramolecular C-H amination of aliphatic azides by dual ruthenium and phosphine catalysis. *Chem. Sci.* **2019**, *10*, 3202–3207. [[CrossRef](#)]
28. Kohler, D.G.; Gockel, S.N.; Kennemur, J.L.; Waller, P.J.; Hull, K.L. Palladium-catalysed anti-Markovnikov selective oxidative amination. *Nat. Chem.* **2018**, *10*, 333–340. [[CrossRef](#)]
29. Zhao, J.; Zhao, X.-J.; Cao, P.; Liu, J.-K.; Wu, B. Polycyclic azetidines and pyrrolidines via palladium-catalyzed intramolecular amination of unactivated C(sp³)-H bonds. *Org. Lett.* **2017**, *19*, 4880–4883. [[CrossRef](#)] [[PubMed](#)]
30. Hennessy, E.T.; Betley, T.A. Complex N-heterocycle synthesis via iron-catalyzed, direct C-H bond amination. *Science* **2013**, *340*, 591–594. [[CrossRef](#)] [[PubMed](#)]
31. Wilding, M.J.T.; Iovan, D.A.; Betley, T.A. High-spin iron imido complexes competent for C-H bond amination. *J. Am. Chem. Soc.* **2017**, *139*, 12043–12049. [[CrossRef](#)] [[PubMed](#)]
32. Bagh, B.; Broere, D.L.J.; Sinha, V.; Kuijpers, P.F.; van Leest, N.P.; de Bruin, B.; Demeshko, S.; Siegler, M.A.; van der Vlugt, J.I. Catalytic synthesis of n-heterocycles via direct C(sp³)-H amination using an air-stable iron(III) species with a redox-active ligand. *J. Am. Chem. Soc.* **2017**, *139*, 5117–5124. [[CrossRef](#)] [[PubMed](#)]
33. Bagchi, V.; Kalra, A.; Das, P.; Paraskevopoulou, P.; Gorla, S.; Ai, L.; Wang, Q.; Mohapatra, S.; Choudhury, A.; Sun, Z.; et al. Comparative Nitrene-transfer chemistry to olefinic substrates mediated by a library of anionic Mn(II) triphenylamido-amine reagents and M(II) congeners (M = Fe, Co, Ni) favoring aromatic over aliphatic alkenes. *ACS Catal.* **2018**, *8*, 9183–9206. [[CrossRef](#)]
34. Lang, K.; Torker, S.; Wojtas, L.; Peter Zhang, X. Asymmetric induction and enantiodivergence in catalytic radical C-H amination via Enantiodifferentiative H-Atom abstraction and stereoretentive radical substitution. *J. Am. Chem. Soc.* **2019**, *141*, 12388–12396. [[CrossRef](#)]

35. Meng, D.; Tang, Y.; Wei, J.; Shi, X.; Yang, M. Copper-catalyzed remote (δ) C(sp³)-H bond amination: A practical strategy to construct pyrrolidine derivatives. *Chem. Commun.* **2017**, *53*, 5744–5747. [[CrossRef](#)]
36. Bagchi, V.; Paraskevopoulou, P.; Das, P.; Chi, L.; Wang, Q.; Choudhury, A.; Mathieson, J.S.; Cronin, L.; Pardue, D.B.; Cundari, T.R.; et al. A versatile tripodal Cu(I) reagent for C-N bond construction via nitrene-transfer chemistry: Catalytic perspectives and mechanistic insights on C-H aminations/amidations and olefin aziridinations. *J. Am. Chem. Soc.* **2014**, *136*, 11362–11381. [[CrossRef](#)]
37. Fiori, K.W.; Espino, C.G.; Brodsky, B.H.; Du Bois, J. A mechanistic analysis of the Rh-catalyzed intramolecular C-H amination reaction. *Tetrahedron* **2009**, *65*, 3042–3051. [[CrossRef](#)]
38. Paradine, S.M.; Griffin, J.R.; Zhao, J.; Petronico, A.L.; Miller, S.M.; White, M.C. A Manganese catalyst for highly reactive yet chemoselective intramolecular C(sp³)-H aminations. *Nat. Chem.* **2015**, *7*, 987–994. [[CrossRef](#)]
39. Zhang, X.; Chung, L.W.; Wu, Y.-D. New mechanistic insights on the selectivity of transition-metal-catalyzed organic reactions: The role of computational chemistry. *Acc. Chem. Res.* **2016**, *49*, 1302–1310. [[CrossRef](#)]
40. Davies, D.L.; Macgregor, S.A.; McMullin, C.L. Computational studies of carboxylate-assisted C-H activation and functionalization at group 8–10 transition metal centers. *Chem. Rev.* **2017**, *117*, 8649–8709. [[CrossRef](#)]
41. Iovan, D.A.; Wilding, M.J.T.; Baek, Y.; Hennessy, E.T.; Betley, T.A. Diastereoselective C-H bond amination for disubstituted pyrrolidines. *Angew. Chem.* **2017**, *129*, 15805–15808. [[CrossRef](#)]
42. Wang, J.; Zhao, C.; Weng, Y.; Xu, H. Insight into the mechanism and site-selectivity of Rh₂^{II,II}(esp)₂-catalyzed intermolecular C-H amination. *Catal. Sci. Technol.* **2016**, *6*, 5292–5303. [[CrossRef](#)]
43. Wang, J.; Zheng, K.; Lin, B.; Weng, Y. A comparative study of inter- and intramolecular C-H aminations: Mechanism and site selectivity. *RSC Adv.* **2017**, *7*, 34783–34794. [[CrossRef](#)]
44. Wang, J. Theoretical Studies on the Mechanisms of C-N/C Formation and Cleavage Promoted by Transition Metal Complexes. Ph.D. Thesis, Sun Yat-sen University, Guangzhou, China, 2010.
45. Wang, J.; Xu, H.; Gao, H.; Su, C.-Y.; Zhao, C.; Phillips, D.L. DFT study on the mechanism of amides to aldehydes using Cp₂Zr(H)Cl. *Organometallics* **2010**, *29*, 42–51. [[CrossRef](#)]
46. Becke, A.D. Density-functional thermochemistry. III. The role of exact exchange. *J. Chem. Phys.* **1993**, *98*, 5648. [[CrossRef](#)]
47. Jang, E.S.; McMullin, C.L.; Käß, M.; Meyer, K.; Cundari, T.R.; Warren, T.H. Copper(II) anilides in sp³ C-H amination. *J. Am. Chem. Soc.* **2014**, *136*, 10930–10940. [[CrossRef](#)] [[PubMed](#)]
48. Wilding, M.J.T.; Iovan, D.A.; Wrobel, A.T.; Lukens, J.T.; MacMillan, S.N.; Lancaster, K.M.; Betley, T.A. Direct comparison of C-H bond amination efficacy through manipulation of nitrogen-valence centered redox: Imido versus iminyl. *J. Am. Chem. Soc.* **2017**, *139*, 14757–14766. [[CrossRef](#)] [[PubMed](#)]
49. Lyaskovskyy, V.; Suarez, A.I.O.; Lu, H.; Jiang, H.; Zhang, X.P.; de Bruin, B. Mechanism of cobalt(II) porphyrin-catalyzed C-H amination with organic azides: Radical nature and H-atom abstraction ability of the key cobalt(III)-nitrene intermediates. *J. Am. Chem. Soc.* **2011**, *133*, 12264–12273. [[CrossRef](#)]
50. Suarez, A.I.O.; Jiang, H.; Zhang, X.P.; de Bruin, B. The radical mechanism of cobalt(II) porphyrin-catalyzed olefin aziridination and the importance of cooperative H-bonding. *Dalton Trans.* **2011**, *40*, 5697–5705. [[CrossRef](#)]
51. Hehre, W.J.; Radom, L.; Schleyer, P.V.R.; Pople, J.A. *Ab initio Molecular Orbital Theory*; Wiley: New York, NY, USA, 1986.
52. Hay, P.J.; Wadt, W.R. Ab initio effective core potentials for molecular calculations. Potentials for the transition metal atoms Sc to Hg. *J. Chem. Phys.* **1985**, *82*, 270. [[CrossRef](#)]
53. Roy, L.E.; Hay, P.J.; Martin, R.L. Revised basis sets for the LANL effective core potentials. *J. Chem. Theory Comput.* **2008**, *4*, 1029–1031. [[CrossRef](#)] [[PubMed](#)]
54. Marenich, A.V.; Cramer, C.J.; Truhlar, D.G. Universal solvation model based on solute electron density and on a continuum model of the solvent defined by the bulk dielectric constant and atomic surface tensions. *J. Phys. Chem. B* **2009**, *113*, 6378. [[CrossRef](#)] [[PubMed](#)]
55. Frisch, M.J.; Trucks, G.W.; Schlegel, H.B.; Scuseria, G.E.; Robb, M.A.; Cheeseman, J.R.; Scalmani, G.; Barone, V.; Mennucci, B.; Petersson, G.A.; et al. *Gaussian 09*; revision D.01; Gaussian, Inc.: Wallingford, UK, 2013.

